Assessment of Natriuretic Peptide Clearance Receptor with Positron Emission Tomography in Cardiovascular Disease Models

Y Liu[1], R Rossin[1], D Abendschein[2], GE Woodard[3], J Zheng[1], K McCommis[1], PK Woodard[1], MJ Welch[1]

[1]Mallinckrodt Institute of Radiology, School of Medicine, Washington University, St Louis, MO, USA
[2]Department of Internal Medicine, School of Medicine, Washington University, St Louis, MO, USA
[3]National Institute of Allergy and Infectious Diseases, Bethesda, MD, USA

Abstract

Cardiovascular molecular imaging is a rapidly evolving field of research, aiming to image and quantify molecular and cellular targets in vivo. Natriuretic peptides (NPs) can acts as a potent inhibitor of vascular smooth muscle cell migration and proliferation through activation of the clearance receptor (NPR-C). In this study, the potential use of a C-type NP fragment (C-ANF) to image the NPR-C receptor expression in developing plaque-like lesions in a rabbit atherosclerosis model and surgically ligated thigh of murine hindlimb ischemia model by functionalization with 1,4,7,10-tetraazacyclo-dodecane-1,4,7,10-tetraacetic acid (DOTA) and labeled with copper-64 for non-invasive imaging with positron emission tomography (PET). Results clearly showed the significantly higher tracer uptake in the injured sites in both models compared to the contralateral control sites. PET imaging and competitive receptor blocking studies demonstrated the NPR-C receptor mediated tracer uptake.

1. Introduction

Cardiovascular disease is the leading cause of death worldwide despite primary and second prevention [1]. Each year more than 1 million people in the United States experience a sudden cardiac event (acute coronary syndrome or sudden cardiac death). Atherosclerosis is a systemic disease characterized by accumulation of lipids, inflammatory cells and connective tissue within the arterial wall. It is a chronic, progressive disease with a long asymptomatic phase. Angiogenesis, defined as the formation of new capillaries by cellular outgrowth from existing microvessels into avascular tissue, is an underlying process in many human disease including cancer, atherosclerotic plaque, and peripheral artery disease etc [2]. To date, many imaging techniques, especially nuclear imaging approach with targeted probes have been developed for atherosclerosis imaging such as fluorine-18-fluorodeoxyglucose ([^{18}F]FDG) [3], [^{99m}Tc] Annexin-V [4] etc, and angiogenesis imaging such as [^{64}Cu]CB-TE2A-c(RGDyK) [5], [^{64}Cu]VEGF$_{121}$ [6] etc. However, the biology of these cardiovascular diseases, provides a number of potential biomarkers for atherosclerosis and angiogenesis imaging [7]. Natriuretic peptides (NPs) are a family of cardiac- and vascular-derived hormones that play a relevant role in cardiovascular homeostasis mainly through the regulation of blood volume and pressure. Among the four group members, the C-type natriuretic peptide (CNP) has a direct effect on immune cell recruitment *in vivo* and is a potent inhibitor of vascular smooth muscle cell migration and proliferation [8]. The NPs exert their antithrombotic effects by interacting with specific cell-surface NP receptors (NPR) [9]. In angiogenesis, the CNP inhibits the production of vascular endothelial growth factor (VEGF) by as much as 88% and endothelia or hypoxia-stimulated VEGF transcription, which is critical for the angiogenesis [10]. Of the three existing NPR's, the 'clearance receptor' (NPR-C) represents approximately 95% of the entire NPR population and is expressed during the growth and remodeling of vascular smooth muscle cells [11].

In this study, we investigate the potential of a CNP fragment, the C-type atrial natriuretic factor (C-ANF) [12] to evaluate the expression of NPR-C receptor in a rabbit atherosclerosis model and murine hindlimb ischemia (HLI) model with positron emission tomography (PET) by conjugating the C-ANF with DOTA and labeled with copper-64.

2. Methods

Synthesis of DOTA-CANF

C-ANF (rat ANF(4-23), Des-Gln^{18},des-Ser^{19},des-Gly^{20,22},des-Leu^{21}) (Bachem, CA) and 1,4,7,10-tetraazacyclododecane-1,4,7,10-tetraacetic acid mono (N-hydroxysuccinimide ester) (DOTA-NHS) (Macrocyclics, TX) conjugation and purification were carried out following standard procedures [13]. The DOTA-conjugated C-ANF was separated from unbound DOTA and from unconjugated peptide by solid phase extraction (C-18 Sep-Pak cartridges, Waters, MA) and reverse phase high performance liquid chromatography (RP-HPLC), respectively. The purified ^{64}Cu-DOTA-C-ANF was concentrated on a Speed-Vac (SC 100, Savant, MN) system equipped with a refrigerated vapor trap (RVT4104, Savant, MN). RP-HPLC was performed on a Dionex system (Dionex, CA) equipped with an UV-Vis detector (Dionex, CA) and a BioScan B-FC-3200 radioisotope detector (BioScan Inc., Washington, DC) on a C-18 analytical column (5 µm, 4.6 mm × 220 mm, Perkin Elmer, MA), with a linear gradient (from 100% H_2O to 65% acetonitrile in 45 min) at a flow rate of 1 ml/min. The UV absorbance was monitored at 210 nm. Under these conditions, C-ANF and DOTA-C-ANF elute from the column at 25.6 and 28.2 min, respectively. The conjugation efficiency was more than 95%, as determined by RP-HPLC. The presence of one DOTA per peptide was confirmed by liquid chromatography – electro spray ionization mass spectrometry (LC-ESI-MS) on a Waters 2695 separation and Micromass ZQ module (Waters, MA).

Copper-64 labeling of DOTA-C-ANF

Copper-64 ($t_{1/2}$ = 12.7h, β^+ = 17%, β^- = 40%) was produced on the Washington University Medical School CS-15 cyclotron by the ^{64}Ni (p,n) ^{64}Cu nuclear reaction at a specific activity of 0.74 - 2.96 GBq /µg at the end of bombardment [14]. DOTA-C-ANF (10 µg, about 5 nmol) was labeled with ^{64}Cu (0.37 GBq) in 200 µL 0.1M ammonium acetate buffer (pH 5.5) at 43 °C for 1 h with a yield of 78.5 ± 4.8% (n = 10). The product was purified on a C-18 sep-pak with solid-phase extraction. The specific activity of the ^{64}Cu-DOTA-C-ANF conjugate was measured as 58.1 ± 3.6 MBq/nmol. The identity of ^{64}Cu-DOTA-C-ANF was confirmed by LC-MS after decay.

Animal preparations to induce atherosclerotic-like lesions

All animal studies were performed in compliance with guidelines set forth by the NIH Office of Laboratory Animal Welfare and approved by the Washington University Animal Studies Committee. Atherosclerotic-like arterial lesions were induced in the right femoral artery of rabbits by air desiccation followed by angioplasty at a later time point, as reported previously [15]. Briefly, male New Zealand White rabbits were fed 0.25% cholesterol-enriched diet throughout the study and elevated serum cholesterol (>200 mg/dL) was confirmed at the time of vessel injury. The right femoral artery was exposed aseptically through a longitudinal skin incision and lidocaine was applied topically to prevent spasm. A 1-2 cm segment of the vessel was isolated between air-tight ligatures and small branches were ligated with suture. A 27-gauge needle was used to puncture the isolated segment proximally as a vent. A second 27-gauge needle was inserted distally into the segment and nitrogen gas was passed through the vessel at a flow rate of 80 mL/min for 8 min to dry and cause sloughing of the endothelium. The segment was then flushed with saline and the ligatures were released to restore blood flow, with gentle pressure applied to the puncture sites for a few minutes to maintain hemostasis. The skin incision was closed and the animal was recovered from anesthesia.

Four to six weeks after the air dessication-induced injury, the lesion site and extent of stenosis in the femoral artery were identified by an angiogram obtained with use of a 4F guide catheter introduced through a carotid arterial cutdown and advanced to the distal aorta. Heparin (100 U/kg, intravenous) was given to prevent clot formation in the catheters. A 0.014 in guidewire was then advanced across the lesion and the guide catheter was removed. A 2.0-2.5 × 20 mm coronary angioplasty balloon was advanced over the guidewire and the site of stenosis was dilated with three, 30 s balloon inflations of 6-8 atm with 1 min between inflations. After re-injuring the lesion site, patency of the femoral artery was confirmed by an angiogram through the angioplasty catheter before the catheter was removed. The carotid was ligated, the skin incision closed, and the animal was recovered from anesthesia. The left femoral artery remained uninjured as a control.

The detail of murine hindlimb ischemia model has been published elsewhere [16]. Briefly, the angiogenesis model used in this study involved ligation of the proximal and distal ends of the right femoral artery, followed by excision of the middle portion of the artery and attached side branches. This created a unilateral ischemia in the mouse hindlimb, followed by slow revascularization of the ischemic muscle, with a significant increase in capillary density, proliferative activity, compared with the left nonischemic muscle.

Imaging protocol

The rabbit atherosclerosis model experimental design is summarized as below. Tracer uptake: nine rabbits (weight = 4.2 ± 0.5 kg) were imaged by MRI and small

animal PET 4-6 weeks after the air dessication-induced injury (time point (TP) 1); six rabbits coming from TP 1 would be imaged by MRI and PET 3 weeks after the balloon overstretching-induced injury (TP 2); four rabbits coming from TP 2 would be imaged by MRI and PET 4 weeks after TP 2 (TP 3). For each PET imaging, about 131 ± 33 MBq (n = 23) of purified ^{64}Cu-DOTA-C-ANF (about 2 nmol) was administered. The baseline tracer uptake was measured in one healthy rabbit (4.6 kg) on a normal rabbit chow diet.

For the HLI model, seven days after the ligation injury, the mice with hindlimb ischemia (n = 4, weight = 23.5 ± 3.6g) were intravenously injected with 0.74 ± 0.08 MBq (n=4) of purified ^{64}Cu-DOTA-C-ANF (about 10 pmol) via the tail vein.

For PET imaging session in both animal models was performed in Focus 220 (Siemens Medical Solutions) with 0-60 min dynamic scan.

The presence of atherosclerotic lesions in the rabbits was confirmed by 3T MRI. T1- (repetition time [TR]/echo time [TE] = 600 ms/12 ms, number of excitations [NEX] = 10 min) weighted turbo-spin-echo images were acquired 1 h after intravenous administration of a non-receptor specific plaque-targeting contrast agent (Gadofluorine M, 0.5 µmol/kg body weight, Bayer Schering Pharma AG, Germany) [16].

For HLI mice, microCT images were acquired on microCAT II (CTI-Imtek) scanner. MicroPET images (corrected for attenuation, scatter, normalization and camera deadtime) and microCT images were co-registered using a landmark registration technique (by using fiducial markers directly attached to the animal bed) and AMIRA image display software (TGS).

Competitive receptor blocking studies were performed on atherosclerotic rabbits (n = 3) and hindlimb ischemic mice (n = 4) by co-injection of ^{64}Cu-DOTA-C-ANF with unlabeled C-ANF peptide with ^{64}Cu-DOTA-C-ANF:C-ANF with 1:100 mole ratio.

3. Results

MicroPET images clearly showed the ^{64}Cu-DOTA-C-ANF tracer uptake at the injury sites with weak uptake observed at non-injured control sites in both rabbit atherosclerosis model and murine HLI model (Figure 1 A and C).

In rabbit atherosclerosis model, at time point 1, the injured femoral artery tracer standardized uptake value (SUV) was 2.01 ± 0.36 (n = 9), significantly different ($p<0.005$) from the control artery tracer SUV of 1.08 ± 0.15 (n = 9). At time point 2, the SUV at injury artery was 1.63 ± 0.29 (n = 6), significantly higher than the tracer uptake at control site (1.10 ± 0.14, n = 6). With unlabeled CANF peptide blocking, the injury artery tracer uptake at time point 2 was decrease to 1.18 ± 0.18 (n = 3) with no statistical difference from the SUV (1.11 ± 0.17, n = 3) of control site, but significantly different ($p<0.05$) from the injured artery SUV in non-blocking studies.

The MR image demonstrated increased signal secondary to Gadofluorine M uptake in the injured rabbit vessel at time point 1 (Figure 1 B). The sites of injury visible on MRI also correlated with regions of increased radiotracer activity seen with PET. The control artery showed no Gadofluorine M uptake.

In mouse HLI model, the injury site SUV was 0.38 ± 0.06 (n = 4), significantly different ($p<0.001$) from the control site tracer uptake (0.17 ± 0.02). With competitive receptor blocking, the SUV at injury site was decreased to 0.15 ± 0.04 (n = 4), with no statistical difference ($p>0.05$) from the uptake at control site (0.13 ± 0.05, n = 4).

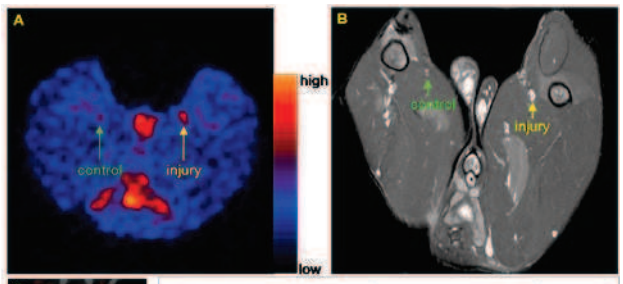

Figure 1 A. Representative transverse PET image of ^{64}Cu-DOTA-C-ANF uptake in rabbit atherosclerosis model at time point 1 showing the accumulation of tracer at injured site
B. Representative transverse MR T1W image of Gadofluorine M accumulation showing a typical atherosclerotic lesion in the femoral artery of a rabbit at time point 1
C. Representative coronal PET/CT fused image of ^{64}Cu-DOTA-C-ANF in mouse HLI model showing the tracer uptake at lesion site

4. Discussion and conclusions

In this study, we demonstrated the capability of a newly developed PET tracer to specifically image the status of the expression of NPR-C receptor regulated on atherosclerotic-like plaques in a rabbit model and murine hindlimb ischemia model. The ^{64}Cu-DOTA-C-ANF tracer uptake at the lesion sites in both models clearly showed the high accumulation, reasonably due to upregulated expression of the NPR-C receptor on the proliferating smooth muscle cells/endothelia.

The competitive receptor blocking studies with excess unlabeled C-ANF peptide decreased the tracer uptakes in the lesion sites to a level similar to that of the control sites in both two models, indicating the tracer uptake at the injury sites were both receptor mediated, indicating

the high specificity of the tracer.

Acknowledgements

We thank Terry Sharp, Paul Eisenbies, Nicole Fettig, Margaret Morris, Amanda Roth, Lori Strong, Ann Stroncek, Jerrel Rutlin and James Kozlowski for their assistance with the imaging studies; Susie Grathwohl for technical help with animal surgery and post-operative monitoring; Tom Voller and Curtis Carey for ^{64}Cu production. This material is based on work supported by the National Institutes of Health as a Program of Excellence in Nanotechnology (HL080729). The production of ^{64}Cu is supported by National Cancer Institute (CA86307).

References

[1] http://www.who.int/mediacentre/factsheets/fs310/en/index.html
[2] Dobrucki LW, Sinusas AJ. Imaging angiogenesis. Current opinion in biotechnology 2007;18:90-6.
[3] Laurberg JM, Olsen AK, et al. Imaging of vulnerable atherosclerotic plaques with FDG-microPET: no FDG accumulation. Atherosclerosis 2007; 192 (2):275-82.
[4] Kolodgie FD, Petrov A, et al. Targeting of apoptotic macrophages and experimental atheroma with radiolabeled annexin V: a technique with potential for noninvasive imaging of vulnerable plaque. Circulation 2003;108:3134-9.
[5] Wei L, Ye Y, et al. ^{64}Cu-labeled CB-TE2A and diamsar-conjugated RGD peptide analogs for targeting angiogenesis: comparison of their biological activity. Nucl Med Biol. 2009;36:277-85.
[6] Willmann JK, Chen K, et al. Monitoring of the biological response to murine hindlimb ischemia with ^{64}Cu-labeled vascular endothelial growth factor-121 positron emission tomography. Circulation 2008; 117:915-22.
[7] Saraste A, Nekolla SG, et al. Cardiovascular molecular imaging: an overview. Cardiovasc Res. 2009; 83:643-52.
[8] Ahluwalia A, Hobbs AJ. Endothelium-derived C-type natriuretic peptide: more than just a hyperpolarizing factor. Trends Pharmacol Sci. 2005;26:162-7.
[9] Scotland RS, Cohen M, et al. C-type natriuretic peptide inhibits leukocyte recruitment and platelet-leukocyte interactions via suppression of P-selectin expression. Proc Natl Acad Sci U S A 2005; 102:14452-7.
[10] Pedram A, Razandi M, et al. Natriuretic peptides suppress vascular endothelial cell growth factor signaling to angiogenesis. Endocrinology. 2001;142:1578-86.
[11] Maack T. Receptors of atrial natriuretic factor. Annu Rev Physiol. 1992;54:11-27.
[12] Maack T, Suzuki M, et al. Physiological role of silent receptors of atrial natriuretic factor. Science 1987;238:675-8.
[13] Rossin R, Muro S, et al. In vivo imaging of 64Cu-labeled polymer nanoparticles targeted to the lung endothelium. J Nucl Med. 2008;49:103-11.
[14] McCarthy DW, Shefer RE, et al. Efficient production of high specific activity 64Cu using a biomedical cyclotron. Nucl Med Biol. 1997;24:35-43.
[15] Sarembock IJ, LaVeau PJ, et al. Influence of inflation pressure and balloon size on the development of intimal hyperplasia after balloon angioplasty. A study in the atherosclerotic rabbit. Circulation 1989;80:1029-40.
[16] Almutairi A, Rossin R, et al. Biodegradable dendritic positron-emitting nanoprobes for the noninvasive imaging of angiogenesis. Proc Natl Acad Sci U S A 2009, 106, 685-90.
[17] Zheng J, Ochoa E, et al. Targeted contrast agent helps to monitor advanced plaque during progression: a magnetic resonance imaging study in rabbits. Invest Radiol. 2008;43:49-55.

Address for correspondence

Yongjian Liu
510 S. Kingshighway Blvd, Campus Box 8225, St Louis, MO 63017, USA